Available online at www.sciencedirect.com
ScienceDirect
Journal of Power Sources 168 (2007) 553–560
JOURNAL OF POWER SOURCES
www.elsevier.com/locate/jpowsour

Characterization methods and modelling of ultracapacitors for use as peak power sources

W. Lajnef*, J.-M. Vinassa, O. Briat, S. Azzopardi, E. Woirgard

Laboratoire IXL CNRS UMR 5818 - ENSEIRB, Université Bordeaux 1, 351 Cours de la Libération, 33405 Talence Cedex, France

Received 8 March 2006; received in revised form 5 January 2007; accepted 15 February 2007
Available online 1 March 2007

Abstract

This paper suggests both a methodology to characterize ultracapacitors and to model their electrical behaviour. Current levels, frequency intervals, and voltage ranges are adapted to ultracapacitors testing. Experimental data results in the determination of the ultracapacitors performances in terms of energy and power densities, the quantification of the capacitance dependence on voltage, and the modelling of the dynamic behaviour of the device. Then, an electric model is proposed taking into account the ultracapacitors characteristics and their future use as peak power source for hybrid and electric vehicles. After, the parameters identification procedure is explained. Finally, the model validation, both in frequency and time domains, proves the validity of this methodology and the performances of the proposed model.

Keywords: Ultracapacitors; Electrical modelling; High current tests; Impedance; Spectroscopy

1. Introduction

Among available storage devices, ultracapacitors exhibit interesting performances for a potential use in hybrid and electric vehicles (HEV). The capacitance of large cells, which is about thousands of Farads, allows the storage of Wh energy with voltage limited to 2.7 V. Thanks to their very low serial resistance (<1 mΩ), they can operate at high levels of instantaneous power. Also, they can work at very low temperatures (down to −40 °C). Additionally, they can support a significant number of charge/discharge cycles. In typical applications as in hybrid and electric vehicles, they can be used as peak power source in combination with a primary source like battery, fuel-cell and generator [1,2].

An analysis of the power requirements in HEV applications and data from literature [3,4] show that the current profiles which are expected to be applied to ultracapacitors are composed of frequent charge and discharge pulses. This is so, because the ultracapacitors are storage devices with finite energy which need to be recharged periodically and because urban driving cycles are discontinuous speed profiles made of repetitive stop-and-go micro-cycles with a typical period around 1–2 min. These charge/discharge pulses are characterized by high current levels, up to 600 A, and a width from about tens of milliseconds to tens of seconds. Following these specificities, we have focused on the dynamic behaviour of ultracapacitors at high current rates. This study is essential for efficient use of these components and to set-up thermal and reliability studies which are key issues in HEV. As ultracapacitors are new devices, their testing methods at high current rates are not well defined. Therefore, we present different methods dedicated to the characterization and the modelling of ultracapacitors at high current rates and the analysis of the corresponding results. Then, we propose an ultracapacitor electrical model adapted to a HEV use. Finally, the parameters identification and the validation of this model on typical current profiles are presented and discussed.

2. Ultracapacitors characterization methods

In this section, different methods are proposed for ultracapacitors characterization and modelling [5–7]. The corresponding tests result in a lot of data and parameters that are very helpful to understand the ultracapacitors behaviour in different frequency intervals and different windows of observation-time. To do so, in this section, we present these tests, their practical

* Corresponding author. Tel.: +33 5 40 00 28 04; fax: + 33 5 56 37 15 45.
E-mail address: lajnef@ixl.fr (W. Lajnef).

0378-7753/$ – see front matter © 2007 Elsevier B.V. All rights reserved.
doi:10.1016/j.jpowsour.2007.02.049

realization and the corresponding results for a Maxwell 2600 F cell BCAP0010. Measurements were conducted using a 0–20 V/±800 A Digatron power tester and an IM6 impedance analyser with a 0–4 V/±40 A PP240 power potentiostat.

2.1. Constant power tests

Constant power tests are commonly used for the characterization of electric storage devices (batteries, flywheel, ultracapacitors, ...) and generators (fuel-cells for instance). For ultracapacitors, the experimental procedure consists in discharging the element with constant power between two voltage limits of U_{nom} and $U_{nom}/2$ in order to measure the specific energy that this element can supply as function of discharge power. As detailed in [8], the corresponding results can be graphically reported in the well-known Ragone diagram where the x-axis and the y-axis correspond, respectively, to the specific power (kW kg^{-1}) and to the specific energy (Wh kg^{-1}). Nowadays, commercially available ultracapacitors have a typical specific power of 4 kW kg^{-1} and a typical specific energy of 6 Wh kg^{-1}. With such performances, they fill the gap between batteries and conventional capacitors.

In practice, to obtain the points corresponding to the maximum of specific power, the tester has to draw out a high current level under low voltage. However, as the time required to obtain these points is small, this maximum current value generally exceeds the peak current reached with repetitive profiles, as for instance, in power cycling tests. According to the specifications given in [5], Fig. 1 shows the Ragone plot obtained for a 2600 F/2.5 V cell and with a specific power that has been limited by the maximum current capability of the tester (800 A). Then, the experimental points have been interpolated and extrapolated according to Eq. (1), where E is the energy, P the power, R the series resistance and C is the rated capacitance [9].

$$E = \frac{C}{2}\left(RP\,\ln\left(\frac{RP}{U_{nom}^2}\right) + U_{nom}^2 - RP\right) \quad (1)$$

This diagram is particularly of interest in order to evaluate the suitability of a given storage device for an application by considering, for instance, the ratio between the specific energy and the specific power. In case of ultracapacitors, these time constants correspond to diagonal lines in Fig. 1 and show that about 6 kW kg^{-1} are available during 0.2 s which is the typical duration for the ignition of the internal combustion engine in stop–start operation in HEV. Then, between 4 and 12 s, more than 1 kW kg^{-1} can be supplied that is interesting for mild-hybrid vehicles.

Finally, these constant power tests confirm that ultracapacitors are convenient for applications that require peak power pulses with short durations of about few seconds as in micro- and mild-hybrids vehicles.

2.2. Constant current tests

Constant current tests represent a basic and a widely used characterization method that is useful to determine the rated capacitance and the equivalent series resistance (ESR). Then, these parameters can be determined both for charge and discharge and for different current levels and ambient temperatures. Therefore, the characterization procedure we have investigated on a 2600 F/2.5 V cell is shown in Fig. 2.

This method is based on a succession of cycles, each made of a constant current charge up to U_{nom} and a constant current discharge down to $U_{nom}/2$, separated by a rest period during which the open-circuit voltage (OCV) is measured.

Fig. 3 illustrates the evolution of the ultracapacitor voltage measured at current switch-off after 200 A constant current charge and discharge with an ambient temperature of 20 °C. This method allows the determination of charge and discharge resistances ESR_c, ESR_d and charge and discharge capacitances C_c, C_d. Their values are given in Table 1 for different current levels.

The results presented in Table 1 show that the ESR and the capacitance decrease with the increasing current level for both charge and discharge. This behaviour can be explained by considering the porous nature of the electrodes which allows to reach a high specific area of capacitive interface. Therefore, this interface can be modelled by a volume distribution of interconnected resistors and capacitors. The higher is the time of charge and discharge, the higher are the accessed resistance and capacitance. As the charge and discharge time decreases

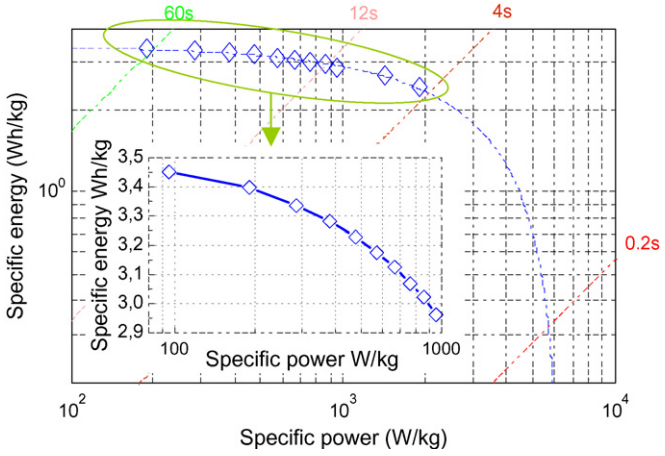

Fig. 1. Ragone plot of a 2600 F cell (obtained with maximum current of 800 A).

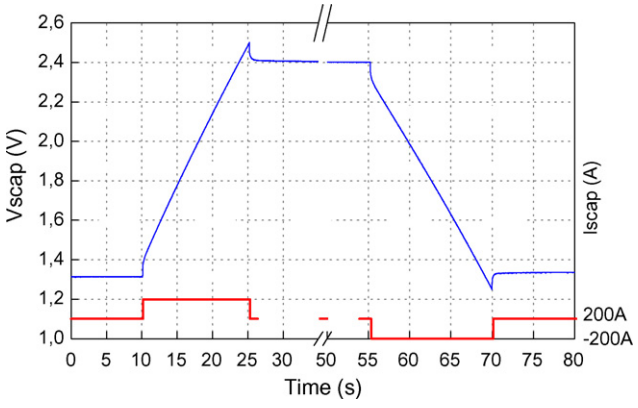

Fig. 2. Experimental voltage response to 200 A charge/rest/discharge current cycle.

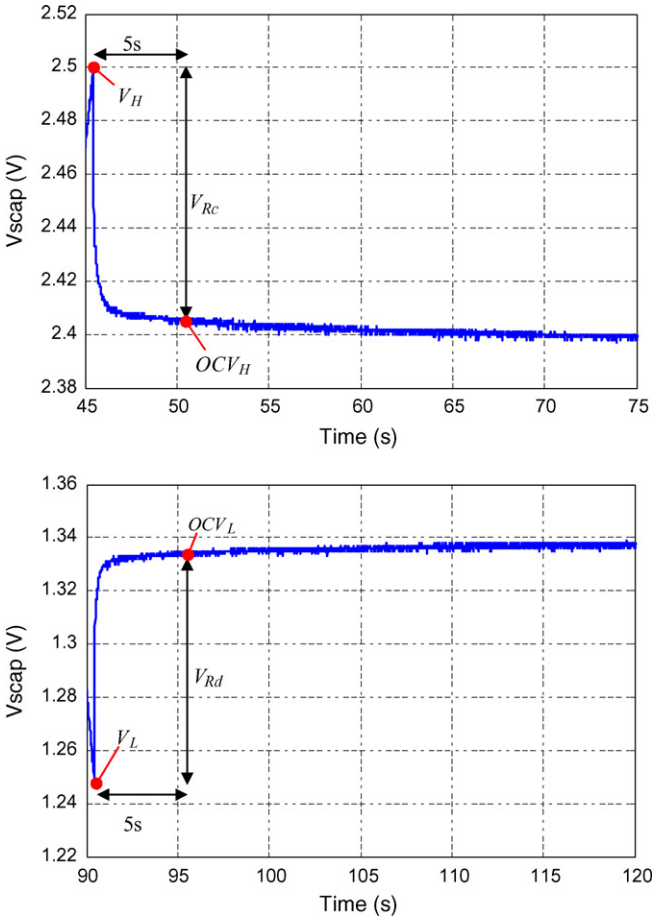

Fig. 3. Open-circuit voltage vs. time following current switch-off after charge (top) and discharge (bottom).

with increasing current level when voltage limits are fixed, the measured capacitance and resistance decrease. In addition, the kinetic behaviour which governs the evolution of the OCV has been analysed and interpreted by considering different electrochemical mechanisms like charge recovery and self-discharge [10].

Then, from these results, we can notice that there is a difference between the charge and discharge ESR values. Consequently, this shows a voltage dependency of the ESR as it was measured from V_L (1.25 V) for ESR_d and from V_H (2.5 V) for ESR_c.

The previously defined and calculated parameters can be associated to a simple electric model, suitable for rough simulations of the dynamic behaviour of ultracapacitors. In addition, the repeatability of this experimental method allows to compare different types of ultracapacitors or to estimate the ageing.

Table 1
ESR and capacitance for different current levels

Current (A)	50	100	150	200
$ESR_c = \frac{V_{Rc}}{I_c}$ (mΩ)	0.53	0.49	0.48	0.47
$ESR_d = \frac{V_{Rd}}{I_d}$ (mΩ)	0.46	0.44	0.43	0.42
$C_c = \frac{I_c \cdot T_c}{OCV_H - OCV_L}$ (F)	2825	2813	2803	2795
$C_d = \frac{I_d \cdot T_d}{OCV_H - OCV_L}$ (F)	2824	2810	2801	2793

In order to develop an enhanced electric model, we have to take into account the voltage dependency of the capacitance [11]. In fact, values of C_c and C_d reported in Table 1 are average capacitances calculated on the whole investigated voltage range. So, let us consider a voltage dependent capacitance. In this case, a differential capacitance C_{diff} is defined by:

$$C_{diff}(v) = \frac{dq}{dv} \tag{2}$$

After a constant current test, the measured capacitance is the mean value of the differential capacitance in the voltage range where the test is done.

$$C = \frac{I(t_f - t_i)}{v_f - v_i} = \frac{1}{v_f - v_i}\int_{v_i}^{v_f} C_{diff}\,dv \tag{3}$$

Now, we suppose that the differential capacitance can be approximated with a polynomial function of voltage.

$$C_{diff} = C_0 + C_1 v + \cdots + C_n v^n \tag{4}$$

For a constant current test, the integral of the differential charge leads to:

$$\int dq = \int C_{diff}\,dv = \int (C_0 + C_1 v + \cdots + C_n v^n)\,dv \tag{5}$$

$$\Delta q = C_0(V - V_i) + \frac{C_1}{2}(V^2 - V_i^2) + \cdots + \frac{C_n}{n+1}(V^{n+1} - V_i^{n+1}) \tag{6}$$

According to the results of constant current tests, we can model the ultracapacitor with a series resistance and a voltage dependent capacitance. Therefore, from Eq. (6), the coefficients C_i can be determined by fitting the charge variation versus the ultracapacitor voltage. Also, the use of the relation $C = I/(\Delta V/\Delta t)$ on small voltage intervals allows the determination of the differential capacitance versus voltage. Subsequently, Fig. 4 shows the variation of the stored charge in Ampere seconds

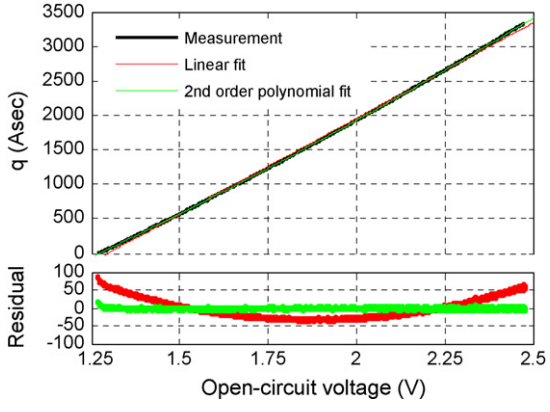

Fig. 4. Cumulated charge (A s) vs. voltage.

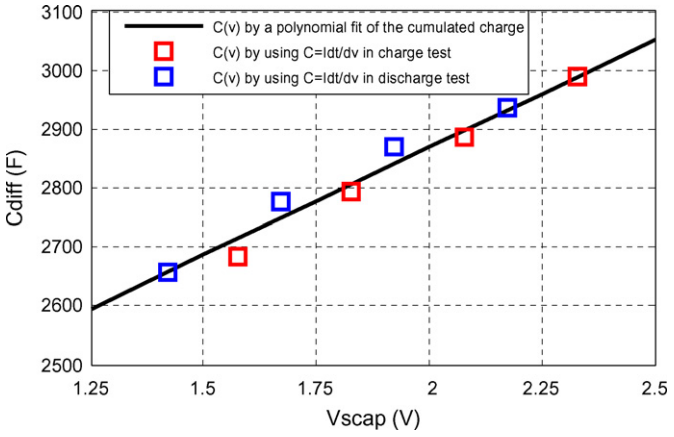

Fig. 5. Capacitance vs. voltage.

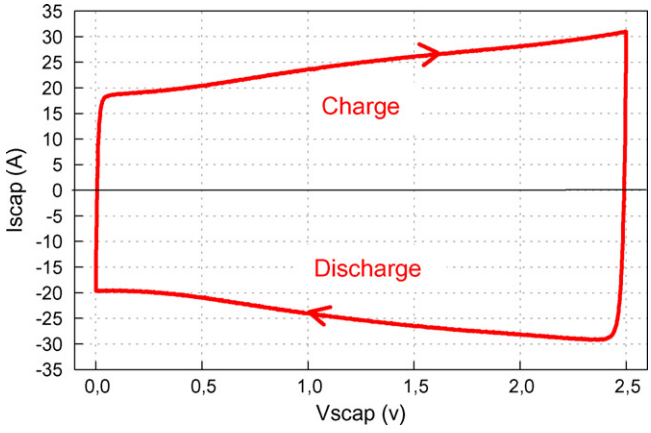

Fig. 6. Voltamogram measured with a sweep rate of 10 mV s^{-1} on a 2600 F/2.5 V cell.

versus the estimated ultracapacitor open-circuit voltage on the intervals of [1.25 V; 2.5 V]. We observe that a second order polynomial function can be used to fit the cumulated charge. Even if the difference with a linear fit is not evident, the residues, which correspond to the difference between measured and calculated points, prove that the second order polynomial function is the best fit. Consequently, we deduce the differential capacitance as a linear function of voltage.

Fig. 5 compares the two methods. The results obtained using the relation $C = I/(\Delta V/\Delta t)$ validate the linear dependency of the capacitance with voltage. Also, they confirm a symmetric behaviour since there is no difference between charge and discharge. Also, Fig. 5 shows that the slope of the capacitance versus voltage curve is about 350 F V^{-1} which represents a more significant dependency than the one due to current level (Table 1). So, this result confirms the importance to take this non-linearity into account.

2.3. Cyclic voltammetry

Cyclic voltammetry is another test method commonly used by electrochemists in order to investigate the properties of electrodes. However, it is extended to ultracapacitors as the electrode/electrolyte interface governs the energy transfer mechanism. This test is useful to validate the capacitive behaviour, to investigate the symmetry between charge and discharge process, and to determine the ultracapacitors potentials limits. It consists of linear voltage sweep between two limit values V_1 and V_2. If the ultracapacitor is modelled with a constant capacitor C in series with an internal resistor R_s, the current is expressed by:

$$I(t) = C\frac{dv}{dt}\left[1 - \exp\left(\frac{-t}{R_s C}\right)\right] \quad (7)$$

In this equation, there are two terms, the first is permanent $I = C dv/dt$, the second is transient and disappears after a few time-constants. When the capacitance depends on voltage and assuming very low serial resistance, the current is proportional to the capacitance by $I = C_{diff} dv/dt$ given that the voltage drop due to the resistor can be neglected.

Fig. 6 illustrates the voltamogram which is obtained by recording the current versus voltage with a sweep rate of 10 mV s^{-1}. This figure shows that the current is constant between 0 and 0.3 V, i.e. the differential capacitance is constant within this voltage range. Then, the current increases as well as the differential capacitance. In the [1.25 V; 2.5 V] range, the linear fit of the differential capacitance which has been determined from constant current tests, seems to be right. Also, the evolution shape of the current versus voltage seems to be symmetric between charge and discharge that corresponds to a reversible behaviour, i.e. the differential capacitance in charge is the same as in discharge.

2.4. Impedance spectroscopy tests

The existing impedance analyzers allow the investigation of a wide frequency range from the μHz to the MHz. But, generally the output current of these apparatus is very low and limited to few hundred of mA. In order to measure very low impedance (<mΩ), voltage variations (in the range of few μV) have to be filtered from a response signal with a large dc bias voltage. These requirements are very difficult to satisfy and the lower is the measured impedance the lower is the accuracy. For this reason, current boosters able to apply high ac currents excitations are used in order to ensure an accurate impedance measurement. In this study, impedance measurements are made with an electrochemical workstation associated with $a \pm 40$ A power booster.

Firstly, Fig. 7 depicts the module and phase of the ultracapacitor impedance versus frequency and Fig. 8 shows the real and imaginary parts versus frequency. The measurements have been done for a 2600 F/2.5 V ultracapacitor in the [1 mHz; 60 kHz] frequency range. The voltage stimulus was characterized by a 10 mV ac peak value and has been applied around 2 V dc bias potential. Consequently, three frequency intervals can be distinguished:

- Very low frequencies (<10 mHz): in this range, the impedance magnitude is relatively high (>5 mΩ). Then, as the phase angle is close to −90°, the ultracapacitor impedance is mainly

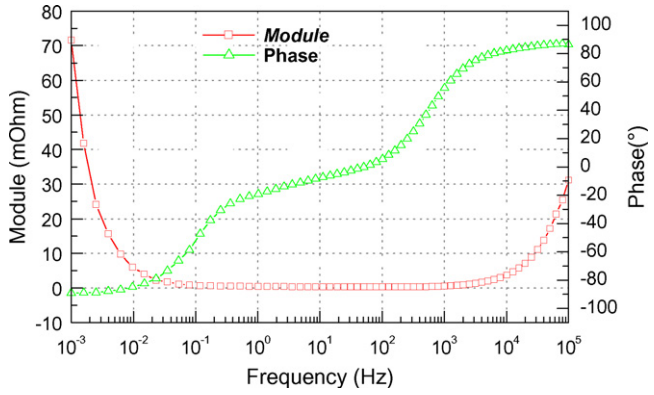

Fig. 7. Module and phase of the ultracapacitor impedance.

capacitive. The particularity of this region is an increase of the real part conversely with frequency which traduces a typical charge redistribution phenomenon [12].

- Medium frequencies [10 mHz; 1 kHz]: we observe that the ultracapacitors behaviour changes from capacitive to inductive. This range is characterized by very low impedance which reaches a minimum value of 0.27 mΩ for a null phase angle. Thus, the ultracapacitors are very convenient to be used as peak power source when the current profiles have their frequency spectrum in this interval.
- High frequencies (>5 kHz): the impedance magnitude is relatively high (>2 mΩ), the phase angle is close to +80° and we notice an inductive behaviour as the impedance real part is increased with the frequency.

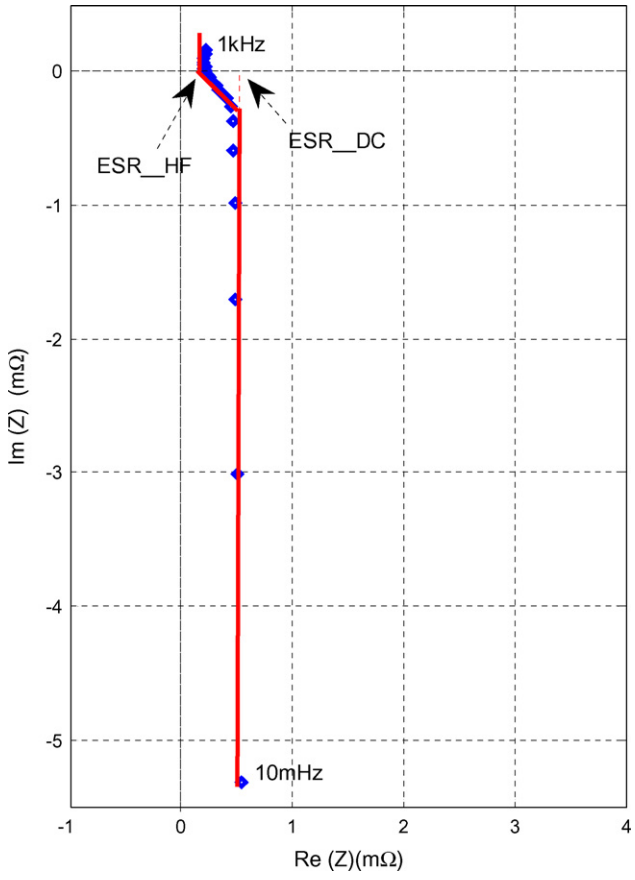

Fig. 9. Nyquist diagram of the ultracapacitor impedance.

Then, we have focused on the impedance in the [10 mHz; 1 kHz] frequency range which is more adapted to their use in HEV applications since the required power pulse will have their frequency spectrum in this interval. Fig. 9 shows this measured impedance in the Nyquist plan.

At low frequencies measurement points follow a vertical line which is the typical Nyquist plot of a pure capacitance in series with a resistance named ESR_{dc}. Then, for intermediate frequencies, the impedance real part decreases with frequency as well as the imaginary part. This behaviour corresponds to the diffusion in a porous electrode and can be approached by an equivalent *RC* transmission line. Finally, beyond a resonance frequency of about 200 Hz, the nature of the impedance changes and becomes inductive whereas the real part tends towards a minimal value, namely ESR_{HF}.

Several measurements have been done at various bias voltages in order to determine the impedance dependency on voltage. As illustrated in Fig. 10, the imaginary part of the impedance, in absolute value, increases when the dc bias potential is reduced. This result traduces a capacitance increase as the voltage increases, as it was previously highlighted thanks

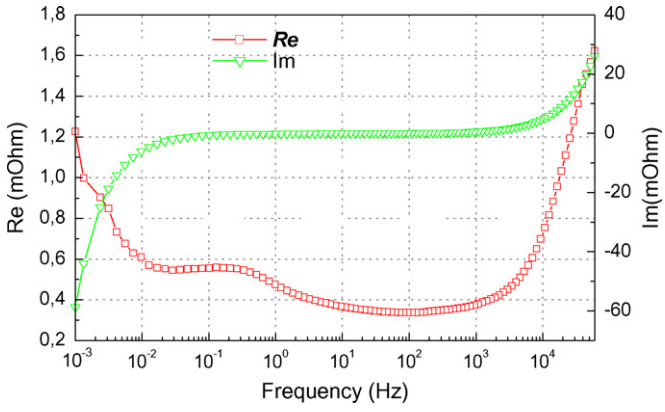

Fig. 8. Impedance real and imaginary parts vs. frequency.

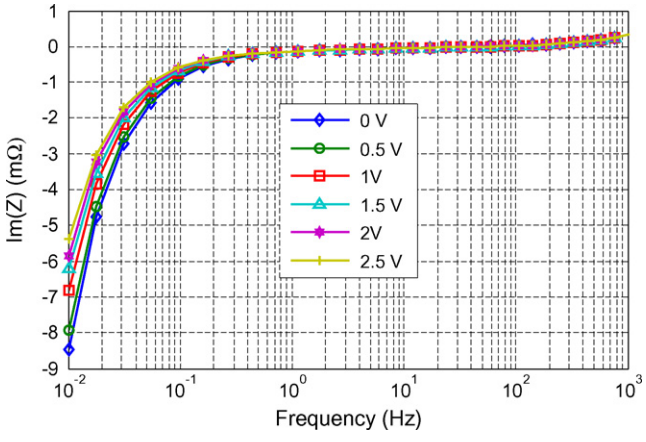

Fig. 10. Impedance imaginary part vs. frequency.

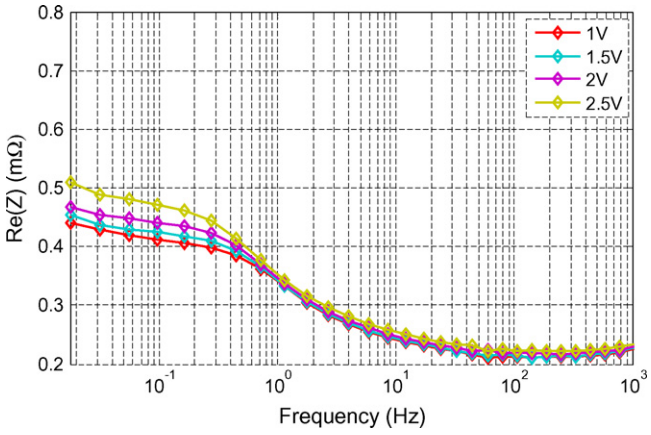

Fig. 11. Impedance real part vs. frequency.

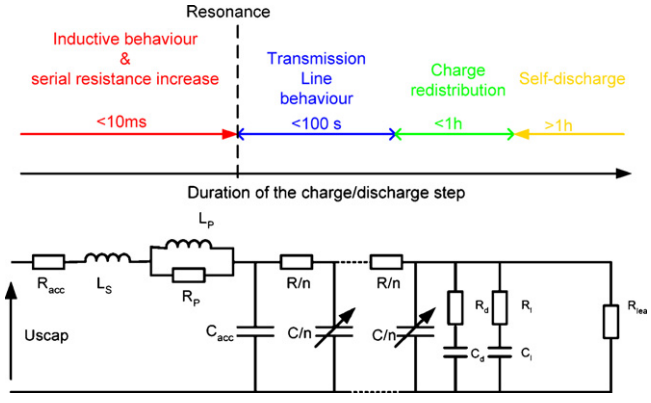

Fig. 12. General electric model of ultracapacitor.

to constant current and cyclic voltammetry tests. Also, as illustrated in Fig. 11, we can notice that the impedance real part at low frequency depends on voltage.

3. Ultracapacitor electrical modelling

3.1. Proposed electric model for ultracapacitors

Different studies were devoted to ultracapacitor modelling [11,13–15]. An overview of these works combined with an analysis of experimental data shows that the ultracapacitor electric model has to take into account many phenomena which are:

- the ultracapacitor behaviour depends on many physical parameters basically voltage and temperature;
- an equivalent *RC* transmission line behaviour that characterizes the ultracapacitors dynamic response especially in the [0.1 Hz; 10 Hz] frequency range. This behaviour is induced by the porous nature of the capacitive interface;
- a resonance frequency (<200 Hz) that corresponds to a transition between capacitive and inductive nature of the impedance and measured at the minimum of the impedance real part;
- an increase of the impedance real part versus frequency and an inductive behaviour above the resonance frequency;
- a charge redistribution phenomenon that occurs at low frequencies or for charge and discharge higher than 1 min. It was modelled by two *RC* branches characterized by long constant times compared with the constant time of the *RC* transmission line;
- a self-discharge which can be modelled by a high parallel resistor called leakage resistor.

Therefore, a general electrical model is proposed in Fig. 12. But, according to the specifications of the application we can neglect some phenomena in order to use the most suitable and the least complicated electric model. In this aim, the window of time-observation of the current and of the voltage that we need for the application is useful. Regarding HEV applications, as previously mentioned, we will focus on the frequency range from 10 mHz to 1 kHz. Therefore, the charge redistribution and the self-discharge phenomena will be neglected. Also, the high frequency behaviour will not be modelled. So, the proposed electric model is given in Fig. 13. It is made of a serial inductor L_s, an access resistor R_{acc} which corresponds physically to the resistance of the device terminals, a capacitor C_{acc} and a non-linear transmission line with voltage dependent capacitors. The impedance real part dependency on voltage is neglected. Finally, the transmission line is approached by *n RC* branches. The higher is the order *n*, the better the dynamic behaviour is modelled.

3.2. Model parameters extraction and validation

The model parameters are identified in different steps using experimental data essentially those obtained from constant current tests and impedance spectroscopy. An identification procedure programmed in Matlab leads to single combination of parameters. At first, we determine the value of the access resistance R_{acc} which corresponds to the minimum of the impedance real part or the magnitude of the measured impedance at the resonance frequency. Then, for frequencies higher than the resonance one, we assume that the transmission line can be neglected. Therefore, the serial inductor L_s and the access capacitance can be extracted by fitting the imaginary part versus frequency. For the tested ultracapacitor, values of 200 F and 50 nH are obtained. Fig. 14 validates the used method by comparing measured points and model results.

Finally, we determine the transmission line parameters *R* and *C*. The transmission line capacitance, *C*, is deduced thanks to the test of charge and discharge with constant currents. In this test, the measured capacitance is the sum of all the capacitance appearing in the electric model. If we neglect the phenomenon of charge redistribution, the measured capacitance will be the sum of C_{acc} and the capacity of the line of transmission *C*. For

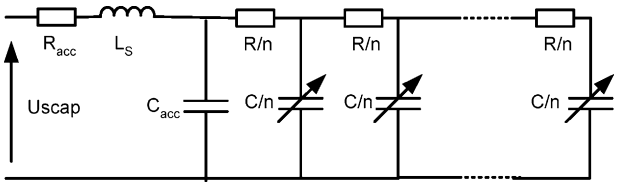

Fig. 13. Ultracapacitor electric model proposed for HEV applications.

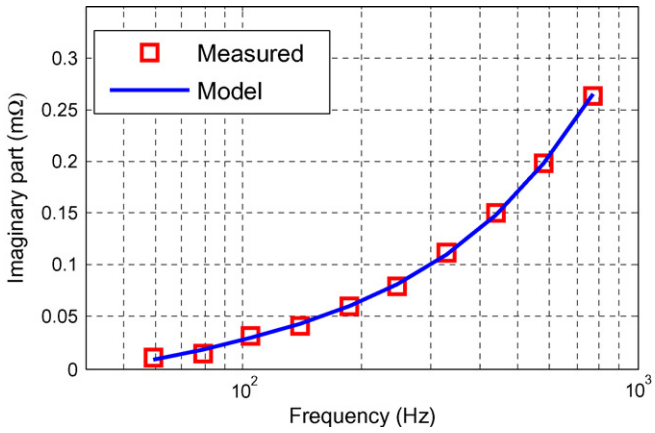

Fig. 14. Comparison of measured and simulated imaginary parts at high frequencies.

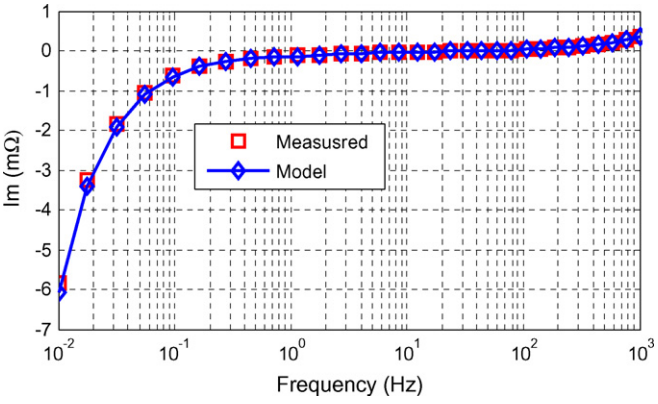

Fig. 15. Model validation in frequency domain: imaginary part vs. frequency.

the tested ultracapacitor, we obtain:

$$C(v)\,[\mathrm{F}] = 2100 + 360 \times V \Rightarrow C = 1900 + 360 \times V$$

The value of the resistance R is determined by fitting the measured real part versus frequency to the impedance real part of the proposed electric circuit. For the tested device we obtain a value of $R = 0.54\,\mathrm{m\Omega}$.

Figs. 15 and 16 validate the proposed model in the frequency domain and in the investigated frequency interval [10 mHz; 1 kHz]. Concerning the transmission line order, good results have been obtained for an order comprised between 4 (Fig. 16) and 20 (Fig. 17). Nevertheless, the user has the possibility to fix the order arbitrary in the identification program.

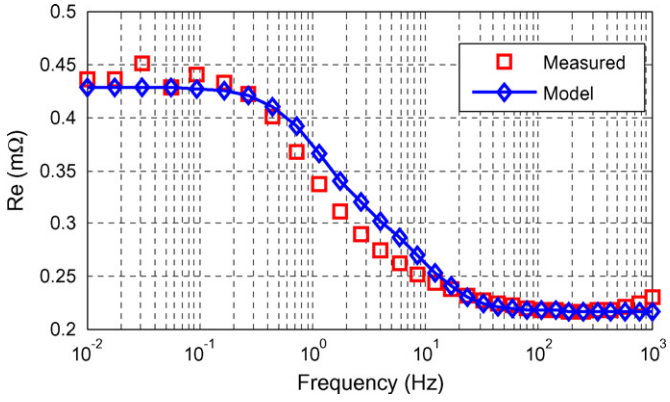

Fig. 16. Model validation in frequency domain: real part vs. frequency (transmission line order = 4).

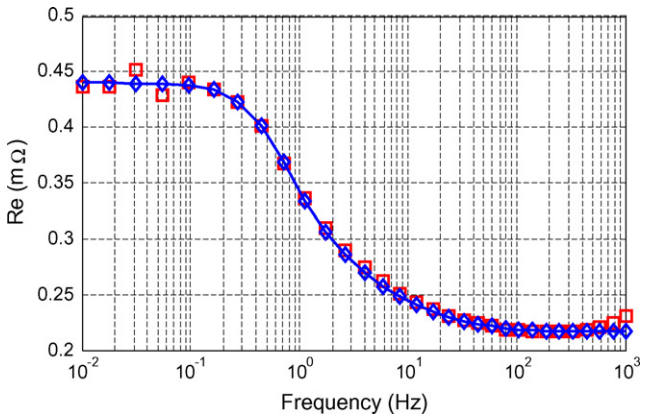

Fig. 17. Model validation in frequency domain: real part vs. frequency (transmission line order = 20).

The dependence of the capacitances with voltage is verified by simulating a cyclic voltammetry. Fig. 18 compares the experimental and simulation results. A difference between simulations and experiments is noticed when the voltage is lower than 0.8 V; then the difference becomes very slight. Indeed, in the model the capacitances values are obtained from constant current tests where the ultracapacitor is charged and discharged between 1.25 and 2.5 V. To enhance the electric model, the capacitances values should be obtained from cyclic voltammetry test. But in this study the model accuracy for voltage low than 1.25 V is not very interesting and so the obtained results are accepted.

Finally, in order to validate the model with high current rate, we have compared the voltage response of the model to the experimental response obtained with a 2600 F/2.5 V cell with a specific current profile made of 200 A charge and discharge pulses. This comparison is illustrated in Fig. 19. By modifying the duration of the charge and discharge pulses, we can estimate the precision of the model for different voltage variations. This result shows that, after 1000 s, there is no global divergence

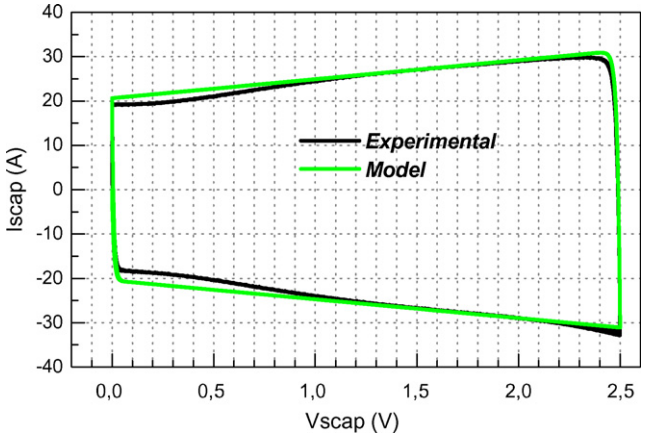

Fig. 18. Cyclic voltamogram: comparison between simulation and experimental results.

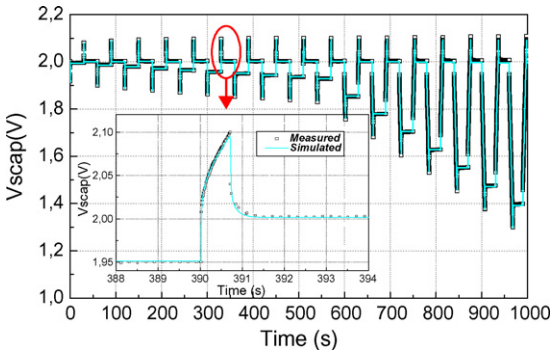

Fig. 19. Model validation with discontinuous current profile (200 A charge and discharge pulses).

between measured and calculated points. Also, we can observe a good matching at the time scale of few seconds.

4. Conclusion

In this paper, ultracapacitors testing methods dedicated to characterization and modelling have been presented. Current levels, frequency intervals and voltage ranges have been defined according to the HEV requirements and the future use of ultracapacitors as peak power devices. Therefore, we have focused on the dynamic behaviour of ultracapacitors and we have noticed that they have a particular behaviour which is essentially capacitive at low frequencies, equivalent to a transmission line at intermediate frequencies, and inductive at high frequencies. Also the capacitance dependence with voltage has been highlighted.

Then, taking into account the ultracapacitors characteristics and the specificities of current profiles, we have proposed a dynamic electric model. The model validation in both frequency and time domains has proved the interest of this methodology and the performances of the model.

The investigation of the ultracapacitors electrical behaviour is a preliminary step before their integration in real applications. The model has to be completed with temperature dependent parameters. This study has to be completed with thermal and reliability studies as high current rates lead to self-heating and ageing.

References

[1] A. Burke, M. Miller, Presented at 19th Electric Vehicle Symposium, EVS'19, Busan, Korea, 2002.
[2] D. Kok, E. Spijker, A. Seibertz, S. Buller, Presented at 18th Electric Vehicle Symposium, EVS'18, Berlin, Germany, 2001.
[3] A. Burke, J. Power Sources 191 (2000) 37–50.
[4] R. Kötz, M. Carlen, Electrochim. Acta 45 (2000) 2483–2498.
[5] A. Burke, J.R. Miller, Presented at Symposium on Electrochemical Capacitors, Chicago, IL, USA, 1995.
[6] Freedom Car Ultracapacitor Test Manual, DOE/NE ID, September 21th 2004.
[7] E. Harzfeld, R. Gallay, M. Hahn, R. Kötz, Presented at 1st European Symposium on Super Capacitors & Applications, Belfort, France, 2004.
[8] W.G. Pell, B.E. Conway, J. Power Sources 63 (1996) 255–266.
[9] T. Christen, M.W. Carlen, J. Power Sources 91 (2000) 210–216.
[10] J. Niu, B.E. Conway, W.G. Pell, J. Power Sources 135 (2004) 332–343.
[11] L. Zubieta, R. Bonert, IEEE Trans. Ind. Appl. 36 (2000) 199–205.
[12] W.G. Pell, B.E. Conway, J. Electroanal. Chem. 500 (2001) 121–133.
[13] F. Belhachemi, S. Raël, B. Davat, Presented at EPE-PEMC, Kosice, Slovak Republic, 2000.
[14] E. Karden, S. Buller, R.W.D. Doncker, Electrochem. Acta 47 (2002) 2347–2356.
[15] W. Lajnef, J.M. Vinassa, S. Azzopardi, O. Briat, E. Woirgard, C. Zardini, J.L. Aucouturier, Presented at PESC04, Aachen, Germany, 2004.